UNIVERSITY OF CALIFORNIA, SAN DIEGO

Dissecting circuit- and stage-specific neural adaptations in an animal model of drug addiction

A thesis submitted in partial satisfaction of the requirements

for the degree Master of Science

in

Biology

by

Cindy Barrientos

Committee in charge:

Professor Byungkook Lim, Chair
Professor Christina Gremel
Professor Nicholas Spitzer

2016

The Thesis of Cindy Barrientos is approved and it is acceptable in quality and form for publication on microfilm and electronically:

Chair

University of California, San Diego

2016

TABLE OF CONTENTS

LIST OF FIGURES

LIST OF TABLES

LIST OF GRAPHS

ACKNOWLEDGEMENTS

I would like to acknowledge Professor Byungkook Lim for his mentorship and guidance as my committee chair, and for giving me the opportunity to learn and grow as a future scientist. I have learned much more than I could have anticipated during my time in this program

I would also like to thank Professor Nicholas Spitzer and Christina Gremel for taking the time to be a part of my committee and working with me through this major step in my career.

Finally, I would like to thank all members of the Lim lab for their support and sharing their knowledge with me, especially Daniel, Eric, Bankole, and Sora.

The research discussed in this thesis is currently being prepared for submission for publication of the material. Barrientos, Cindy; Knowland, Daniel. The thesis author and Daniel Knowland were the primary investigators and authors of this material.

ABSTRACT OF THE THESIS

Dissecting circuit- and stage-specific neural adaptations in an animal model of drug addiction

by

Cindy Barrientos

Master of Science in Biology

University of California, San Diego, 2016

Professor Byungkook Lim, Chair

Drug addiction is a major global health problem, persisting due to a lack of effective treatments. This is largely due to insufficient understanding of the pathophysiology and neural circuitry underlying the progression of a healthy individual into drug addiction. Rodent models of cocaine addiction implicate the altered activity of medium spiny neurons (MSNs) in the nucleus accumbens (NAc) in the progression to addiction. MSNs of the NAc can be classified as

dopamine receptor D1 or D2 expressing neurons, and cocaine exposure has previously been shown to induce differential changes in these two cells types, including differential modifications of dendritic spine densities and different changes in synaptic plasticity. While the neural substrates driving these changes remain unknown, it is possible that synaptic changes driven by the neural adaptation in the regions upstream of the NAc may have roles in response to cocaine administration. Therefore, we seek to determine whether brain areas sending major excitatory projections to the NAc MSNs exhibit morphological changes during different stages of cocaine exposure. In particular, previous work has shown the roles of basolateral amygdala (BLA), prefrontal cortex (PFC), and the ventral hippocampus (VH) projections to the NAc in facilitating behavioral aspects of addiction. We utilized a method of monosynaptic retrograde tracing using an EnvA pseudotyped rabies virus that would allow us to label neurons in these areas that directly project to MSNs. The effect of cocaine on spine density was measured in multiple stages: initial use (5 days of cocaine exposure), withdrawal (5 days of cocaine followed by a 2 week withdrawal period without cocaine), and reinstatement (5 days of cocaine followed by a single cocaine reinstatement shot at the end of 2 week withdrawal). Here, we characterize the distinct effects of cocaine exposure on dendritic modifications in a projection-, cell type-, and stage-specific manner. Our findings suggest cocaine differentially alters spine densities on neurons in brain areas that send excitatory projections to different types of NAc MSNs. These neuroanatomical results establish a

framework to further understand the circuit-basis of progression to drug addiction.

Introduction

Drug abuse is one of the major public mental health issues in the United States, at best leading to decreased productivity and health decline; at worst, drug abuse leads to crime, dismantling of families, and preventable deaths. In particular, cocaine abuse has been increasing in college-aged Americans, as past-year use has increased by over 60% from 2013 to 2014 alone (Johnson 2015). Furthermore, relapse rates may be as high as 60% in the year following treatment for those who may attempt to quit an addictive substance (McLellan 2000). Unfortunately, effective treatments have not yet been developed, due in large part to our lack of knowledge in the mechanisms of the progression to and relapse of drug addiction. As such, it is crucial to understand the mechanisms leading to drug addiction to create strategies to prevent and treat this devastating condition.

Nucleus accumbens

The nucleus accumbens (NAc), deemed one of the “pleasure centers” of the brain, is a major player in processing reward-related behaviors, and has been heavily implicated in drug addiction (Dackis 2001). Indeed, rats have been shown to compulsively press a lever that delivers the electrical stimulation of the NAc, similar to compulsive drug-seeking behavior in addicted humans (Olds and Milner 1954).

The NAc predominantly consists of medium spiny neurons (MSNs) that express either dopamine receptor D1 (D1-MSN) or dopamine receptor D2 (D2-MSN). These two subtypes of MSNs were traditionally believed to be separated into the direct (D1-MSNs) and indirect (D2-MSNs) pathway: D1-MSNs in the NAc project directly to basal ganglia output nuclei, including the ventral tegmental area (VTA), whereas D2-MSNs in the NAc predominantly project indirectly to the VTA by relaying signals through the ventral pallidum (VP) (Gerfen 2011). However, it has recently been determined in mice that D1-MSNs project to both the VTA and VP, while D2-MSNs predominantly project to VP (Kupchik 2015). Although these two MSN subtypes are not as distinct in their projection targets as once believed, they do carry opposing functions: D1-MSNs promote appetitive behaviors, while D2-MSNs motivate aversion (Richard 2011). Optogenetic activation of D1-MSNs during a cocaine condition placed preference test (CPP) increases cocaine reward compared to a low dose of cocaine alone, while activation of D2-MSNs attenuates the rewarding effects of higher doses of cocaine (Lobo 2010). Interestingly, even after rodents have reached a point of compulsive drug taking, optogenetically increasing the activity of NAc D2-MSNs is still able to significantly decrease their motivation for cocaine seeking (Bock 2013). Overall, it is believed that drug addiction is in part due to the disruption of the balance between D1-MSN and D2-MSN activity.

Glutamatergic inputs to the nucleus accumbens

In addition to receiving dopaminergic projections from the ventral tegmental area (VTA), NAc MSNs are also modulated by major excitatory inputs, including projections from the prefrontal cortex (PFC), the basolateral amygdala (BLA), and the ventral hippocampus (VH) (Britt 2012). These projections are known to be associated with different phenotypes of addiction-related behaviors: the PFC is involved in decision-making and behavioral inhibition – two functions that are stunted in those plagued with addiction (Stuss and Levine 2002). One group developed the “Iowa gambling task” to test a subjects’ decision-making abilities and found patients with ventromedial PFC damage were unable to consider future implications of their actions and instead followed immediate gratification (Bechara 1994). The PFC is also necessary for the induction of behavioral sensitization to cocaine; this sensitization is the phenomenon in which each subsequent exposure to cocaine induces increased locomotion in the minutes after drug administration (Steketee 2005). Lesions of the PFC by ibotenic acid injections have been shown to prevent behavioral sensitization in rodents (Pierce 1997).

Substructures of the PFC are also known to be affected differently with exposure to cocaine: prolonged cocaine use leads to decrease excitability in the prelimbic (PrL) neurons, and countering PrL hypoactivity by optogenetic activation of PrL neurons suppresses compulsive cocaine seeking resistant to shock treatment (Chen 2013). Prior studies found that damage to the PrL

attenuated the acquisition of cocaine-induced CPP, as well as the reinstatement of cocaine-induced CPP after extinction training (Tzschentke and Schmidt 1998, Zavala 2003). The onset of behavioral sensitization to cocaine has been shown by one group to require the PrL, as lesions prevent locomotor sensitization (Tzschentke 1998).

A different PFC substructure, the orbitofrontal cortex (OFC), has been found to express increased ΔFosB after chronic cocaine administration. Exogenous overexpression of ΔFosB in the OFC dramatically increased voluntary cocaine intake in rats when compared to control. In addition, the higher expression of ΔFosB led to increased impulsivity in rats using a 5-choice serial reaction time task (5CSRT) test measuring premature responses (Winstanley 2009). An fMRI study on human addicts have implicated the OFC in cocaine seeking behaviors, as the subjects exhibited increased glucose metabolism in the OFC – indicative of increased neural activity - in proportion to the extent of cocaine craving (Volkow and Folwer 2000). The medial portion of the OFC (MO) has been associated with a preference for immediate rewards, as an fMRI study found increased activity in the MO of humans during behavioral tasks leading to immediate availability of money; this finding was later supported by a rat lesion study, in which damage to the MO led to a decrease in preference for a small, immediate reward over a large, delayed reward. (McClure 2004, Mar 2011)

The BLA has been implicated in cocaine-seeking behavior, as lesions to the BLA in naïve rodents prevent the acquisition of cocaine-induced CPP, while

the same lesions in cocaine-induced CPP acquired animals prevented extinction of CPP and cocaine-seeking; this suggests the BLA encodes incentive values, and damage to this region impairs the ability to re-assess the value of cocaine-paired stimuli (Fuchs 2002). The BLA's ability to facilitate cocaine seeking extends even after extinction training of rats that learned to lever press for cocaine infusions, as electrical stimulation of the BLA is sufficient to induce cocaine seeking (Hayes 2003). In addition, BLA-lesioned rats have a diminished freezing response to cues associated with a footshock, indicating predictable negative consequences are less likely to inhibit drug seeking (Pelloux 2013).

The BLA is not the only glutamatergic input to the NAc that is involved in cocaine seeking after extinction training; electrical stimulation of the VH has been found to induce a relapse to cocaine seeking after extinction (Vorel 2001). Vice versa, lidocaine inactivation of the VH decreases relapse to cocaine seeking (Sun 2003). The same dose of lidocaine injected in to the BLA also decreases cocaine reinstatement post-extinction training, indicating some overlapping function in behavioral outputs of the BLA and VH (Kantak 2002). The VH also encodes contextual cues of cocaine intake, as chemical inactivation of the VH attenuates context-induced reinstatement of cocaine-seeking (Lasseter 2010).

Dendritic spines

Spines are dendritic protrusions and the major targets of excitatory projections. They are commonly found throughout the brain and are known to be involved in synaptic formation and maturation (Nimchinsky 2002). Furthermore,

their morphological alterations are observed in the pathogenesis of many neurological diseases, including autism spectrum disorders (ASD), schizophrenia, and Alzheimers disease (Penzes 2011).

Spines can be divided into three different subtypes based on morphological criteria: thin, mushroom, and stubby. Stubby spines are typically short and lack a thin neck connecting the head to the dendrite. Stubby spines are quite common in the early developing brain, though it is not known how or why. Mushroom spines are named as such because of its thin neck leading to a bulbous head. Mushroom spines are controversially thought to be matured thin spines, with a stronger synapse due to its greater post-synaptic density (PSD). Thin spines have a long and narrow neck with a small diameter head. Thin spines are considered to be the most plastic of the three, as they may form and recede rapidly within minutes to hours, although, mushroom spines are known to be quite plastic as well as they may recede or become other spine types. Thin spines that are immature are transient unless it connects with an afferent to form a synapse (Nimchinsky 2002). Because the spine head is proportional to the area of the PSD and the quantities of postsynaptic receptors and presynaptic docked vesicles, the larger spine heads – such as in mushroom and stubby spines – are associated with stronger synaptic transmission; this allows experimenters to indirectly measure synaptic strength in the brain by spine density and subtype analysis (Hering 2001).

Several studies have demonstrated cocaine's ability to alter dendritic spine densities on MSNs, indicating the drug may re-organize connectivity of excitatory inputs to the NAc. Even after a 28 day withdrawal, cocaine-induced spine density decreases in the NAc core still persists, showing long lasting plasticity that may be associated with some aspect of long lasting addiction phenotypes (Dumitriu 2012). A recent study found that short-term 5 day cocaine exposure is able to specifically increase the spine density of D1-MSNs in the NAc that receive projections from the BLA, while inducing no effect on D1-MSNs that receive projections from the ventral hippocampus (MacAskill 2014). The implications of differential effects on excitatory projections to the NAc MSNs are particularly important, given the different behavioral outputs of each of these projections to the NAc.

In consideration of changes in dendritic spines as highly associated with the maturational and functional status of synapses, we are interested in determining whether these changes in the dendritic spine densities of NAc MSNs also occur in upstream regions that send glutamatergic inputs to the NAc, as these projections are believed to be responsible for many of the addiction-related behaviors. Despite the importance of experience-dependent structural plasticity related to the progression to drug addiction, it has not yet been studied systematically. Therefore, we propose a new experimental design to determine whether cocaine is able to induce specific changes in primary glutamatergic

projections to either D1- or D2-MSNs of the NAc at different stages in the progression to addiction.

Experimental Scheme for cocaine administration and imaging

Drug addiction is a progressive disorder: it is initiated by recreational use, and with frequent and persistent use will develop into compulsive drug seeking and abuse. It is often characterized by periods of prolonged abstinence, withdrawal, and relapse. To address how cocaine may induce morphological changes in different brain areas at different stages of this progression, we designed a mouse model to mimic these separate stages of cocaine exposure. Initial prolonged drug use will be studied by injecting mice with 20 mg/kg of cocaine once a day for 5 days. To test for changes during a period of abstinence following drug exposure, another group of mice will be injected with cocaine once a day for 5 days before undergoing 14 days of no cocaine exposure. The mouse will then be given a saline challenge injection on day 15. Because relapse is incredibly common in drug addicts, we decided to mimic the reinstatement of drug exposure by injecting 5 days of cocaine into mice, followed by 14 days of withdrawal and a cocaine challenge on day 15.

After the cocaine administration phase is complete, the animals are sacrificed to obtain brain slices containing the medial orbitofrontal prefrontal cortex (MO), PrL, BLA, and VH with EGFP-labeled neurons. Once mounted onto microscope slides, the brain slices will be imaged on a confocal microscope. Once GFP-labeled cells are identified, secondary dendritic branches are imaged;

8-10 images of dendrites are acquired per brain area per animal and are deconvolved prior to spine analysis (including spine density quantification and spine morphological subtype classification).

Viral strategy

To label the inputs specific to D1-MSNs and D2-MSNs, we utilized a monosynaptic retrograde viral tracing technique together with transgenic mice expressing Cre recombinase specifically in D1-MSNs (D1-Cre) or D2-MSNs (A2a-Cre). To restrict retroviral infection to Cre-expressing neurons and monosynaptically-connected afferent neuronal populations, we used a strategy using a combination of several viruses. By co-infecting Cre-expressing cells in the NAc with separate adeno-associated viruses (AAV) that conditionally express 1) TVA and the marker protein tdTomato (AAV-DIO-tdTOM-TVA) and 2) RVG (AAV-DIO-RVG), we enable expression of tdTomato, TVA, and RVG only in Cre-expressing neurons. Then, we used a rabies viral vector (SADΔG-EGFP(EnvA)), which is initially incapable of retrograde transport as it lacks the requisite rabies glycoprotein (RVG). The rabies viral vector is then pseudotyped with EnvA such that it can only infect cells that express exogenous avian leukemia virus receptor A (TVA; Wickersham et al. 2007). Thus, a subsequent injection of the EnvA pseudotyped rabies virus (SADΔG-EGFP(EnvA)) will yield expression and trans-synaptic labelling of the rabies marker protein only in Cre and tdTomato-expressing neurons.

Methods

Animals

All animal housing and handling were conducted under the ethical standards of University of California IACUC. Adult male and female A2a-cre and D1-cre mice were obtained from GENSAT (Gene Expression Nervous System Atlas) and backcrossed with wild type C57BL mice. Mice were group-housed for the duration of the experiments, and maintained on a 12hr light/dark cycle (lights on at 7am). Animals were randomly assigned to either control or experimental groups. Surgeries were performed between 10-12 weeks of age. In D1-cre mice, 6 were exposed to 5 day saline injections, 6 were exposed to 5 day cocaine injections, 6 were exposed to a saline reinstatement shot after 5 days of cocaine and a 14 day withdrawal, and 7 were exposed to a cocaine reinstatement shot after 5 days of cocaine and a 14 day withdrawal. In A2a-cre mice, 6 were exposed to 5 day saline injections, 5 were exposed to 5 day cocaine injections, 7 were exposed to a saline reinstatement shot after 5 days of cocaine and a 14 day withdrawal, and 7 were exposed to a cocaine reinstatement shot after 5 days of cocaine and a 14 day withdrawal.

Surgeries

Mice were anaesthetized with a 150mg/kg ketamine and dexmedetomidine mixture i.p. injection. Viruses were stereotaxically injected (Kopf Instruments) using a Harvard Apparatus syringe pump into the right NAc

core with coordinates relative to bregma: anterior/posterior +1.5, medial/lateral +1.0, dorsal/ventral -4.4. The syringe was left for ten minutes after viral administration to minimize potential leakage dorsal of the injection site via syringe removal. The scalp was immediately resealed using 3M Vetbond Tissue Adhesive. Mice were then injected i.p. with 150 mg/kg Antisedan and s.c. with 100 µl of buprenorphine and maintained on a heating pad during recovery from anaesthesia.

For 5 day cocaine group and saline control group, two helper viruses, AAV-DIO-tdTom-TVA and AAV-DIO-RVG (150 nl each), were injected unilaterally into the right NAc core 14 days prior to the first cocaine injection. Two days prior to the first saline habituation injection, SADΔG-EGFP(EnvA) was injected into the same location and the animal is sacrificed one day after the final cocaine injection. These regiments ensured robust expression of SADΔG-EGFP(EnvA) while minimizing the risk of potential cell death induced by longer periods of viral expression.

For withdrawal groups, two helper viruses, AAV-DIO-tdTom-TVA and AAV-DIO-RVG (150 nl each), were injected into the NAc core 2 days prior to the first saline habituation injection. Then, 6 days before the reinstatement shot, SADΔG-EGFP(EnvA) was injected into the same location and the animal was perfused the day following reinstatement. Refer to figure 1 for a diagrammatic representation.

Histology

Mice were perfused 24 hours after the last cocaine or saline injection. First, animals were anaesthetized with isoflurane gas and perfused with 0.9% saline solution, followed by 4% paraformaldehyde (PFA) in phosphate-buffered saline (PBS). Brain was fixed overnight in 4% PFA at 4°C. After wash with PBS, the brain was sectioned into 50 µm coronal slices on a Leica VT1000s vibratome and immediately mounted on Superfrost plus microscope slides with DAPI Fluoromount-G.

Behavioral sensitization test

All groups of animals underwent a habituation period in which saline was i.p. injected into animals once per day in the two days prior to the sensitization test and placed into a 27.25 x 27.25 cm open field arena used for monitoring locomotion. Animals were re-weighed each day prior to behavior in order to account for potential fluctuations in weight and subsequent changes in cocaine concentration administration. After each saline or cocaine injection (20 mg/kg), the animal is immediately placed into the chamber to monitor locomotion by BIOBSERVE software for 15 minutes (Graph 1).

For 5 day repetitive cocaine administered group and saline control, animals were injected daily for 5 consecutive days at the same time ± 2 hours. The animals were sacrificed 24 hours later.

For withdrawal groups, animals were injected daily for 5 consecutive days at the same time ± 2 hours and monitored for locomotor sensitization. The animals then underwent a 2 week withdrawal in their home cage in which no saline or cocaine was administered. After 2 weeks withdrawal, a single 20 mg/kg cocaine or saline challenge (cocaine reinstatement and saline reinstatement groups, respectively) shot was administered. Animals were again sacrificed 24 hours later.

Imaging

Secondary dendrites were imaged under an Olympus Fluoview FV1200 confocal microscope using a 100x lens at 3.5x zoom with a resolution of 1024x1024 in which each pixel corresponded to 0.035 x 0.035 x 0.15 µm. Z-stacks were acquired on FV10-ASW software. A highly sensitive gallium arsenide phosphide (GaAsP) detector was used in most cases to ensure visualization of all spines. For more accurate quantitation and future morphological analysis, images were processed with AutoQuant X3 deconvolution software prior to analysis.

Spine quantitation

Deconvolved images were imported and analyzed through NeuronStudio (Rodriguez 2008). The software allows for automated spine counting; however, to ensure optimal and accurate counting, a human experimenter would manually verify each spine. This software also allows for automated, unbiased counting of

dendritic spine subtypes (thin, mushroom, and stubby). All imaging and quantitation was performed blind to the experimental condition and genotype.

Statistical analysis

Graphpad Prism was utilized for all statistical tests. Dendritic spine densities were calculated by dividing total spines by length of the dendritic segment analyzed. Spine subtype ratios were calculated by dividing the number of spine subtype by total spines. Statistical differences of dendritic spine density between cocaine exposed animals and those given 5 days of saline injections were determined using a K-S test, as well as the Mann-Whitney (depicted in the bar graphs). Mann-Whitney was also used to compare spine subtype ratios of cocaine exposed groups to saline control.

Results

BLA neurons projecting to NAc MSNs are differentially affected by cocaine

Our results indicate that BLA neurons projecting to D1-MSNs and D2-MSNs showed distinct changes in dendritic spine density at different stages of cocaine administration. First, there is an increase in the dendritic spine density of D1-MSN projecting BLA neurons after 5 days of cocaine injections, and continues to increase after 14 days of withdrawal (fig. 2B). The ratio of MSN spine subtypes of BLA neurons projecting to D1-MSNs exhibit a decrease in the fraction of thin spines and an increase in that of mushroom spines after 5 days of cocaine and after a 14 day withdrawal; this indicates that thin spines are matured into mushroom spines after 5 days of cocaine injections and during a withdrawal period (fig. 2D). Cocaine reinstatement after 14 days of withdrawal returns spine density levels near that of 5 day cocaine exposure. This may be due to the decrease in the fraction of mushroom spines and increase in that of thin spines after the cocaine reinstatement, suggesting that the mushroom spines generated during the withdrawal period are more plastic than those increased during the 5 day cocaine injections.

Second, BLA neurons projecting to D2-MSNs show no change in spine density by cocaine injections, indicating that cocaine administration induces specific structural plasticity in BLA neurons based on their projections. However, there is rearrangement of all three spine subtype ratios: there is an increase in thin spines after saline reinstatement, and a decrease in mushroom spines

across all groups compared to control (fig. 2G). We also observe an increase in stubby spines after 5 days of cocaine exposure and cocaine reinstatement. It's possible that despite no net change in the dendritic spine density of D2-MSN projecting BLA neurons, individual spines display dynamic changes in response to cocaine administration.

Spine density increases in VH neurons projecting to D1- but not D2-MSNs with a cocaine challenge after 14 days of withdrawal

Hippocampal projecting neurons contain long and elaborated dendritic structures (fig. 3A). Moreover, the different areas of dendrites receive inputs from different brain structures. Thus, we hypothesized that these differences may lead to selective changes in spine densities between dendrite subtypes – apical and basal dendrites – in response to cocaine administration. We found that 5d cocaine administration showed no change in spine density on apical and basal dendrites of VH neurons projecting to D1-MSNs. Interestingly, the increases in dendritic spines were observed only after a cocaine challenge, not by a saline challenge, following a 14 day withdrawal period with greater changes in the apical dendrites than the basal. The fraction of different subtypes of dendritic spines remains consistent across all groups in the apical dendrites, suggesting that all subtypes of spines increased after a cocaine challenge following a 14 day withdrawal period (fig. 3D). However, basal dendrites undergo a decrease in the ratio of stubby spines after a 14 day withdrawal with a saline challenge, and

decrease even further after a cocaine reinstatement shot, suggesting a selective increase in thin and mushroom spines after cocaine withdrawal.

Similar to the BLA-NAc projections, VH neurons projecting to D2-MSNs show no change in dendritic spine density in response to cocaine administration. Furthermore, cocaine does not induce any changes in spine subtype ratios in the apical dendrites of VH neurons projecting to D2-MSNs (fig. 4D). Interestingly, we find a significant decrease in thin spines after 5 days of cocaine injections in the basal dendrites, indicating that the dynamics of thin spine maturation is altered by cocaine administration (fig. 4G).

Cocaine induces spine density decreases in dendrites of PrL inputs to D1-MSNs, but not D2-MSNs

Like VH neurons, NAc projecting layer 5 PrL neurons also have long, elaborated dendritic structures. Thus, we examine the spine in apical and basal dendrites separately. Contrary to D1-MSN projecting neurons in the BLA and VH, cocaine induces a decrease in the spine density of PrL cells innervating NAc D1-MSNs (fig. 5A). Apical dendrites exhibit a significant decrease in spine density after a 14 day withdrawal with a saline or cocaine challenge (fig. 5B, 5C). Aside from a short term increase in stubby spines after 5 days of cocaine exposure, there are no changes in spine subtype ratios (fig. 5D). More pronounced decreases in spine density are observed in basal dendrites of Prl neurons projecting to D1-MSNs in all 3 cocaine-administered groups (fig. 5E). The average spine density of the basal dendrites decreases after 5 day cocaine

exposure; this effect continues to persist after 14 days of withdrawal with a saline or cocaine reinstatement shot (fig. 5F). No change in spine subtype composition in basal dendrites was observed.

Unlike changes in spine density of PrL neurons projecting to D1-MSNs in response to cocaine administration, no change was observed in the spine density in both apical and basal dendrites of cells projecting to D2-MSNs upon cocaine administration (fig. 6B, 6C, 6E, 6F). Despite no net changes in density, there is structural reorganization of individual spines given the alterations in thin and stubby spine ratios: apical dendrites exhibit a decrease in thin spines and an increase in stubby spines after 5 days of cocaine injections. Thin spines on basal dendrites also decrease after 5 days of cocaine exposure, however, stubby spines increase after 5 days of cocaine and is retained after withdrawal and reinstatement. Since stubby spines are also considered immature, there may be a recession of thin spines that is replaced by new stubby spines.

Cocaine decreases the spine density of basal dendrites on MO neurons projecting to D1-MSNs after withdrawal, and also causes decreases in MO neurons projecting to D2-MSNs after initial 5 day cocaine use

The MO and the PrL, collectively known as the prefrontal cortex, are known to carry different functions. For this reason, we decided to subdivide these regions in our analysis in the event that cocaine may also differentially affect them. Indeed, this was found to be the case (fig. 7A). The dramatic decreases in spine density with 5 days of cocaine exposure to PrL cells were not seen in the

MO; apical dendritic spine density of D1-MSN projecting MO neurons were unaffected by cocaine (fig. 7B, 7C). However, spine rearrangement may be occurring as a significant decrease in thin and increase in mushroom spines are seen after 14 days of cocaine withdrawal, suggesting that thin spines may be maturing into a mushroom-type structure, or that there is a recession of thin spines that is replaced by growth of new stubby spines (fig. 7D). Basal dendrites of these cells show a decrease in spine density after a 14 day cocaine withdrawal with a saline reinstatement shot (fig. 7E)). These effects appear to recover after a cocaine reinstatement shot (fig. 7F). Spine subtype ratios remain mostly consistent across all groups; however, there is an increase in mushroom spines after 14 day cocaine withdrawal. It may be that the spine densities after withdrawal and saline reinstatement were non-selectively decreased, and the recovery seen after a cocaine reinstatement is due to an induction of mushroom spine synaptogenesis.

Of all four D2-MSN projecting brain areas analyzed, only MO inputs to D2-MSNs show cocaine-induced changes in spine density (fig. 8A). Apical dendrites undergo a significant decrease in spines after 5 days of cocaine exposure, though, a recovery occurs after 14 day withdrawals – regardless of a saline or cocaine reinstatement shot (fig 8B, 8C). Significant spine subtype rearrangement is also induced: there is a decrease in thin spines after 5 days of cocaine, as well as an increase in stubby subtypes in all cocaine exposed groups (fig. 8D). 5 days of cocaine exposure also induces a decrease in spine density of basal dendrites

(fig. 8E); though the effect is lost after a 14 day withdrawal, regardless of saline or cocaine reinstatement. Spine subtype ratio alterations are similar across apical and basal dendrites: there is a decrease in thin spines after 5 days of cocaine, while an increase is observed in stubby spines across all cocaine exposed groups (fig. 8G). This indicates that regardless of whether cocaine has recently been taken or 14 days prior, the drug is able to increase the proportion of stubby spines in both types of dendrites.

Figures

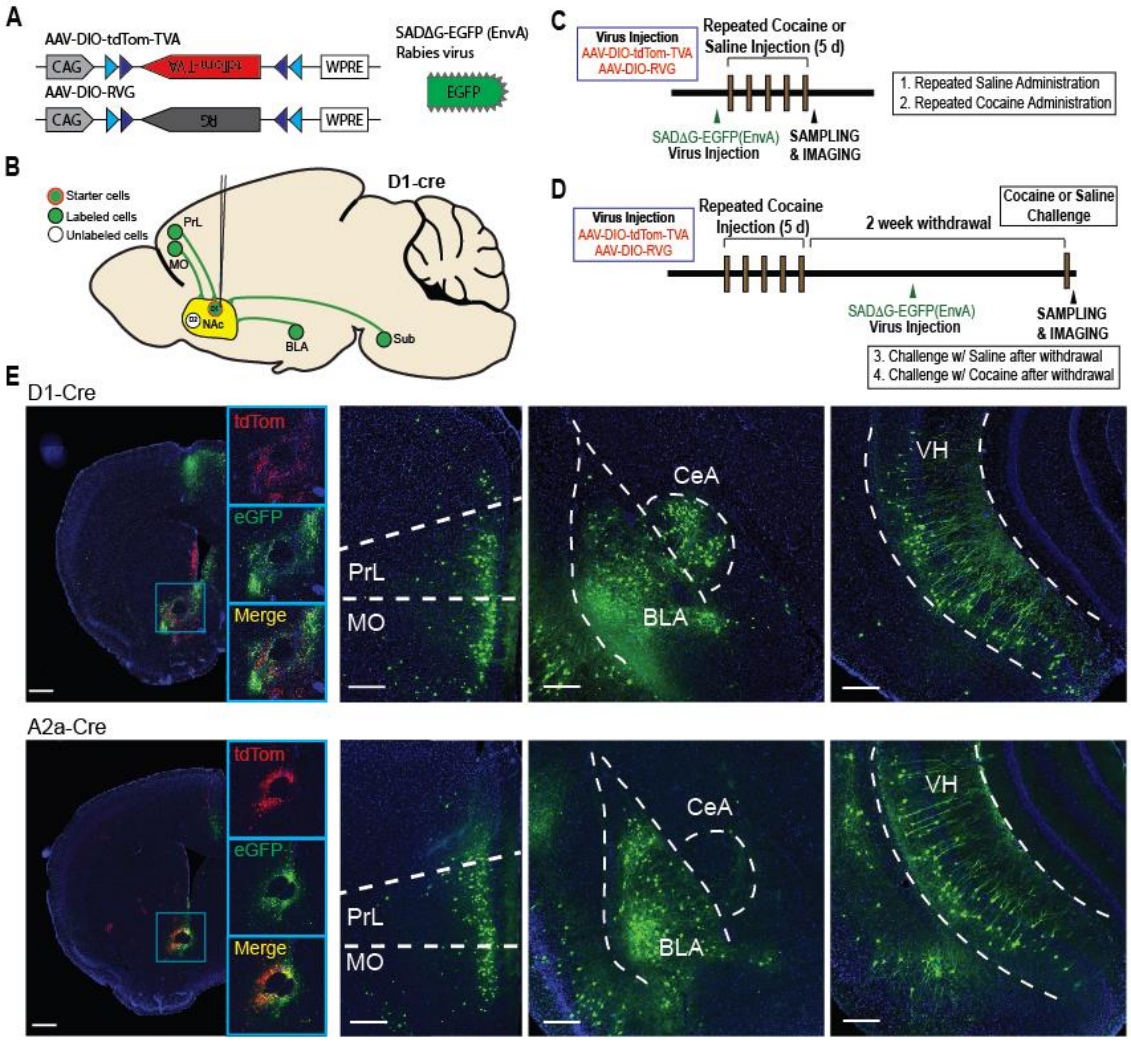

Figure 1. Experimental scheme. **A**) Two helper viruses, AAV-DIO-tdTom-TVA and AAV-DIO-RVG are injected into the NAc of either D1- or A2a-cre animals to selectively express red fluorescence, rabies glycoprotein, and a TVA receptor in cre-expressing cells. A pseudotyped rabies virus (SADΔG-EGFP (EnvA)) is injected into the same site 14 days later and able to infect cre-expressing cells containing the TVA receptor to retrogradely label neurons that form synapses directly onto the TVA-expressing cre cells. **B**) Representation of a D1-Cre mouse brain indicating the site of viral injections (the NAc), and the retrograde EGFP labeling into neurons of the PrL, MO, BLA, and VH that directly project onto D1-MSNs of the NAc. **C**) Timeline for 5d C and control animals. **D**) Timeline for 14WD S and 14WD C animals. **E**) From left to right. Top: NAc injection site in an A2a-cre animal with zoomed in channel separation of tdTom and EGFP; D2-MSN projecting neurons from the PrL and MO, the BLA and CeA, and the VH. Bottom: NAc injection site in a D1-cre animal with zoomed in channel sepration of tdTom and EGFP; D1-MSN projecting neurons from the the PrL and MO, the BLA and CeA, and the VH. Scale bars of injection sites represent 1 mm, while those in projection regions represent 250 µm.

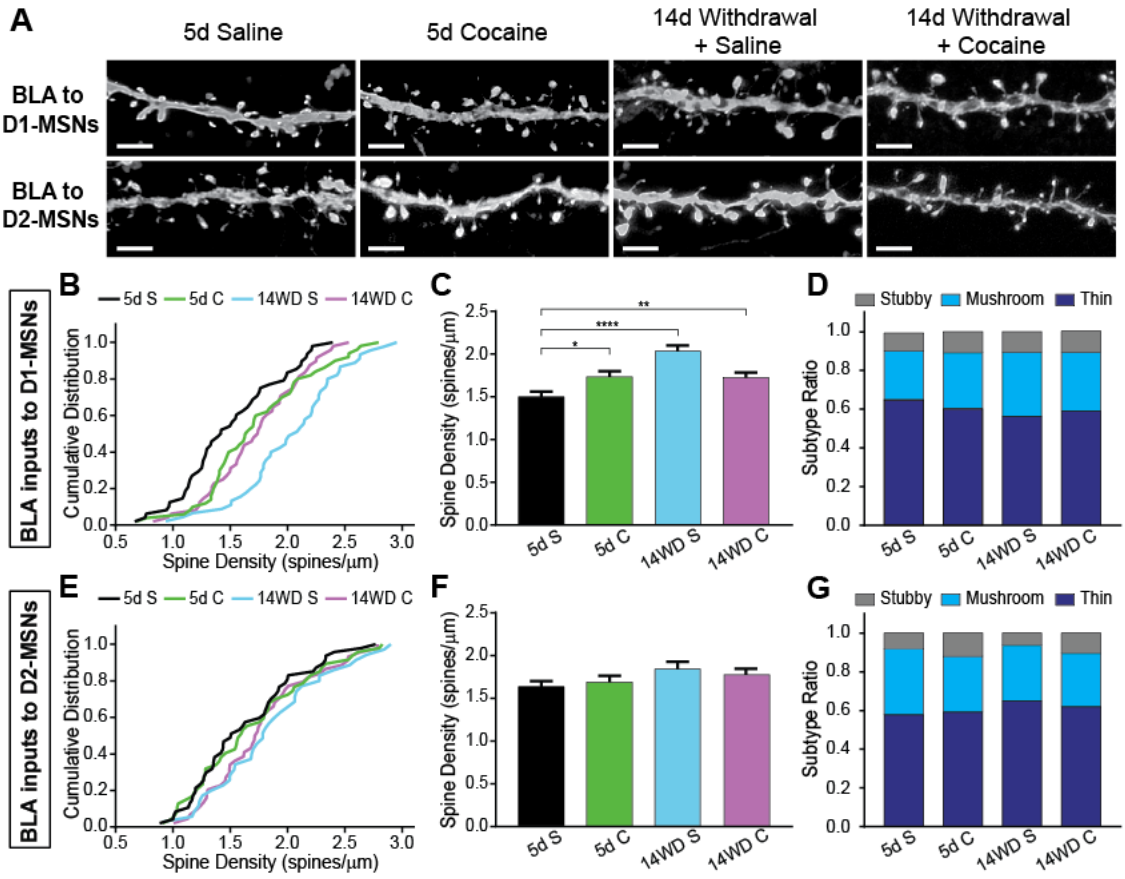

Figure 2. Selective increases in dendritic spine density of BLA neurons projecting to D1-MSNs, but not D2-MSNs, of the NAc after chronic cocaine exposure, withdrawal, and reinstatement. **A**) Sample images of dendrites from BLA neurons projecting to D1-MSNs (top) and D2-MSNs (bottom) in different stages of cocaine administration. Scale bars represent 1 µm. **B**) Cumulative distribution of dendritic spine density of BLA neurons projecting to D1-MSNs (5d S: n = 48; 5d C: n = 50, p = 0.0143; 14WD S: n = 45, p < 0.0001; 14WD C: n = 48, p = 0.0337 when compared to 5d S); K-S test. **C**) Average spine density of dendritic spines analyzed in **B** with s.e.m (5d S: 1.418 ± 0.06332; 5d C: 1.645 ± 0.06783, p = 0.0133; 14WD S: 2.081 ± 0.06726, p <0.0001; 14WD C: 1.74 ± 0.05838, p = 0.0084 when compared to control, Mann-Whitney test. **D**) Stacked column chart depicting changes in average spine subtype ratios of BLA neurons projecting to D1-MSNs (5d S: n = 40; 5d C: n = 38; 14WD S: n = 45; 14WD C: n = 40). **E**) Cumulative distribution of dendritic spine density of BLA neurons projecting to D2-MSNs (5d S: n = 47; 5d C: n = 47, n.s.; 14WD S: n = 35, n.s., 14WD C: n = 44, n.s. when compared to 5d S). **F**) Average spine density of dendritic spines analyzed in **E** with s.e.m (5dS: 1.507 ± 0.06785; 5d C: 1.596 ± 0.07553, p = 0.6789; 14WD S: 1.784 ± 0.08522, p = 0.0674; 14WD C: 1.726 ± 0.06921, p = 0.1524. **G**) Stacked column chart depicting changes in average spine subtype ratios of BLA projections to D2-MSNs (5d S: n = 31; 5d C: n = 38; 14WD S: n = 35; 14WD C: n = 44). Each n signifies a dendrite analyzed from 4-6 animals. *p<0.05, **p<0.005, ****p<0.0001

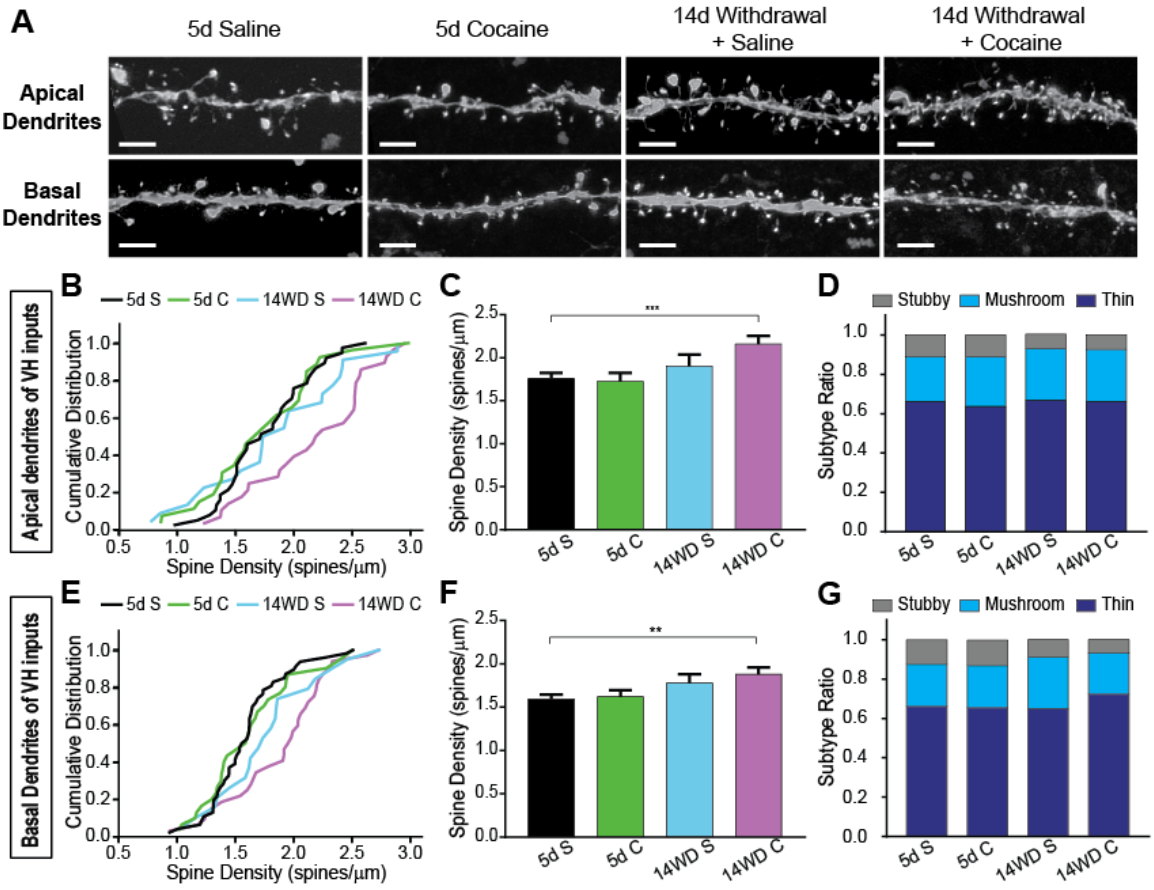

Figure 3. Cocaine reinstatement increases spine densities of apical and basal dendrites of VH neurons projecting to D1-MSNs of the NAc. **A**) Sample images of apical (top) and basal (bottom) dendrites from VH neurons projecting to D1-MSNs in different stages of cocaine administration. Scale bars represent 1 µm. **B**) Cumulative distribution of apical dendritic spine density of VH neurons projecting to D1-MSNs (5d S: n = 37; 5d C: n = 26, p = 0.9828; 14WD S: n = 23, p = 0.4672; 14WD C: n = 28, p = 0.0045 when compared to 5d S); K-S test. **C**) Average spine density of dendritic spines analyzed in **B** with s.e.m (5d S: 1.76 ± 0.06383; 5d C: 1.726 ± 0.09773, p = 0.7238; 14WD S: 1.903 ± 0.1355, p = 0.3487; 14WD C: 1.966 ± 0.09579, p = 0.0010 when compared to 5d S, Mann-Whitney test. **D**) Stacked column chart depicting changes in average apical spine subtype ratios of VH neurons projecting to D1-MSNs (5d S: n = 37; 5d C: n = 26; 14WD S: n = 25; 14WD C: n = 23). **E**) Cumulative distribution of basal dendritic spine density on VH projections to D1-MSNs (5d S: n = 46; 5d C: n = 30, p = 0.9232; 14WD S: n = 19, p = 0.1316, 14WD C: n = 32, p = 0.0009. when compared to 5d S); K-S test. **F**) Average spine density of dendritic spines analyzed in **E** with s.e.m (5d S: 1.595 ± 0.04862; 5d C: 1.623 ± 0.07353, p = 0.9874; 14WD S: 1.778 ± 0.1013, p = 0.0875; 14WD C: 1.883 ± 0.07525, p = 0.0013. **G**) Stacked column chart depicting changes in average basal spine subtype ratios of VH neurons projecting to D1-MSNs (5d S: n = 46; 5d C: n = 30; 14WD S: n = 20; 14WD C: n = 23). Each n signifies a dendrite analyzed from 4-6 animals. *p<0.05, **p<0.005, ****p<0.0001.

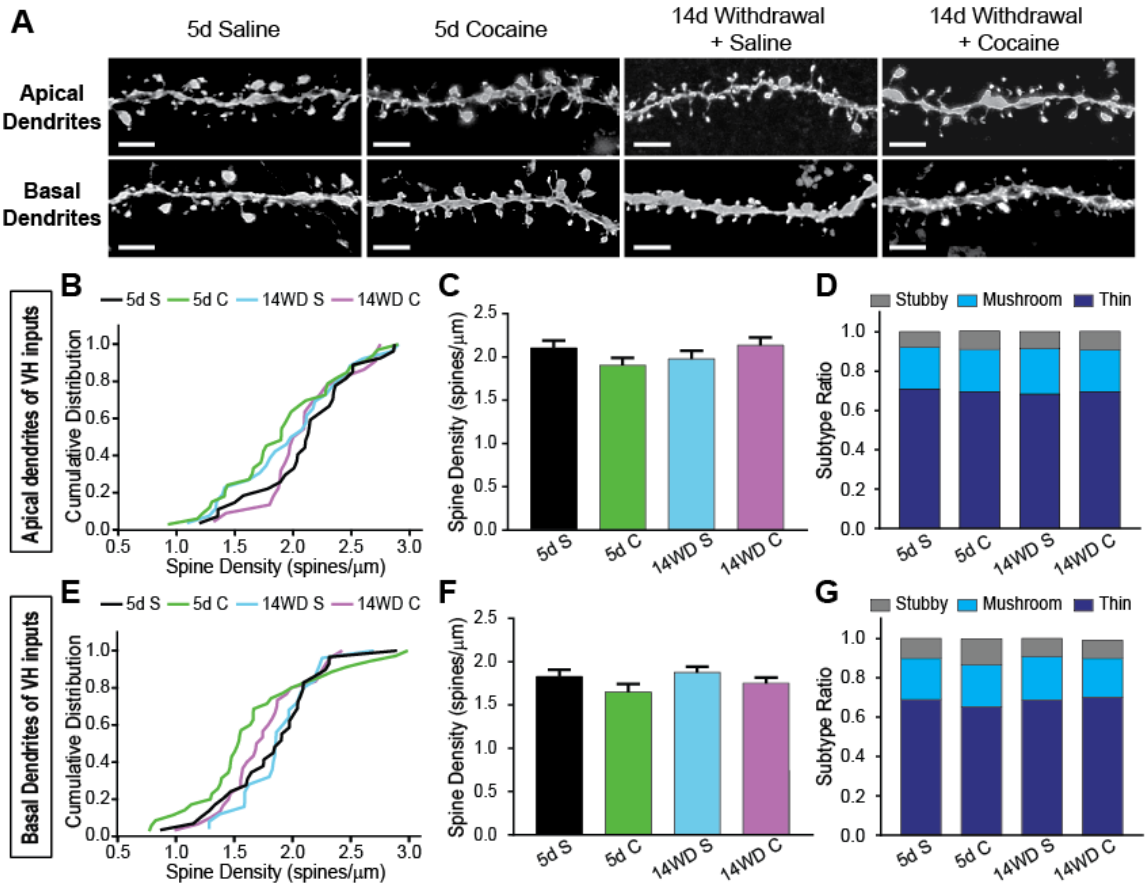

Figure 4. Cocaine exposure does not change spine densities of apical and basal dendrites of VH neurons projecting to D2-MSNs of the NAc in any of the experimental groups. **A**) Sample images of apical (top) and basal (bottom) dendrites from VH neurons projecting to D2-MSNs in different stages of cocaine administration. Scale bars represent 1 µm. **B**) Cumulative distribution of apical dendritic spine density of VH neurons projecting to D2-MSNs (5d S: n = 27; 5d C: n = 33, p = 0.0894; 14WD S: n = 26, p = 0.06417; 14WD C: n = 23, p = 0.6956 when compared to 5d S); K-S test. **C**) Average spine density of dendritic spines analyzed in **B** with s.e.m (5d S: 2.103 ± 0.08504; 5d C: 1.904 ± 0.08628, p = 0.0876; 14WD S: 1.978 ± 0.09646, p = 0.3441; 14WD C: 2.134 ± 0.08868, p = 0.7576 when compared to 5d S, Mann-Whitney test. **D**) Stacked column chart depicting changes in average apical spine subtype ratios of VH neurons projecting to D2-MSNs (5d S: n = 27; 5d C: n = 34; 14WD S: n = 26; 14WD C: n = 23). **E**) Cumulative distribution of basal dendritic spine density of VH neurons projecting to D2-MSNs (5d S: n = 29; 5d C: n = 35, p = 0.0502; 14WD S: n = 25, p = 0.9698, 14WD C: n = 30, p = 0.3127. when compared to 5d S); K-S test. **F**) Average spine density of dendritic spines analyzed in **E** with s.e.m (5d S: 1.828 ± 0.07906; 5d C: 1.652 ± 0.0926, p = 0.0705; 14WD S: 1.878 ± 0.0652, p = 0.8634; 14WD C: 1.753 ± 0.06467, p = 0.3538. **G**) Stacked column chart depicting changes in average basal spine subtype ratios of VH neurons projecting to D2-MSNs (5d S: n = 29; 5d C: n = 35; 14WD S: n = 25; 14WD C: n = 30). Each n signifies a dendrite analyzed from 4-6 animals. *p<0.05, **p<0.005, ****p<0.0001

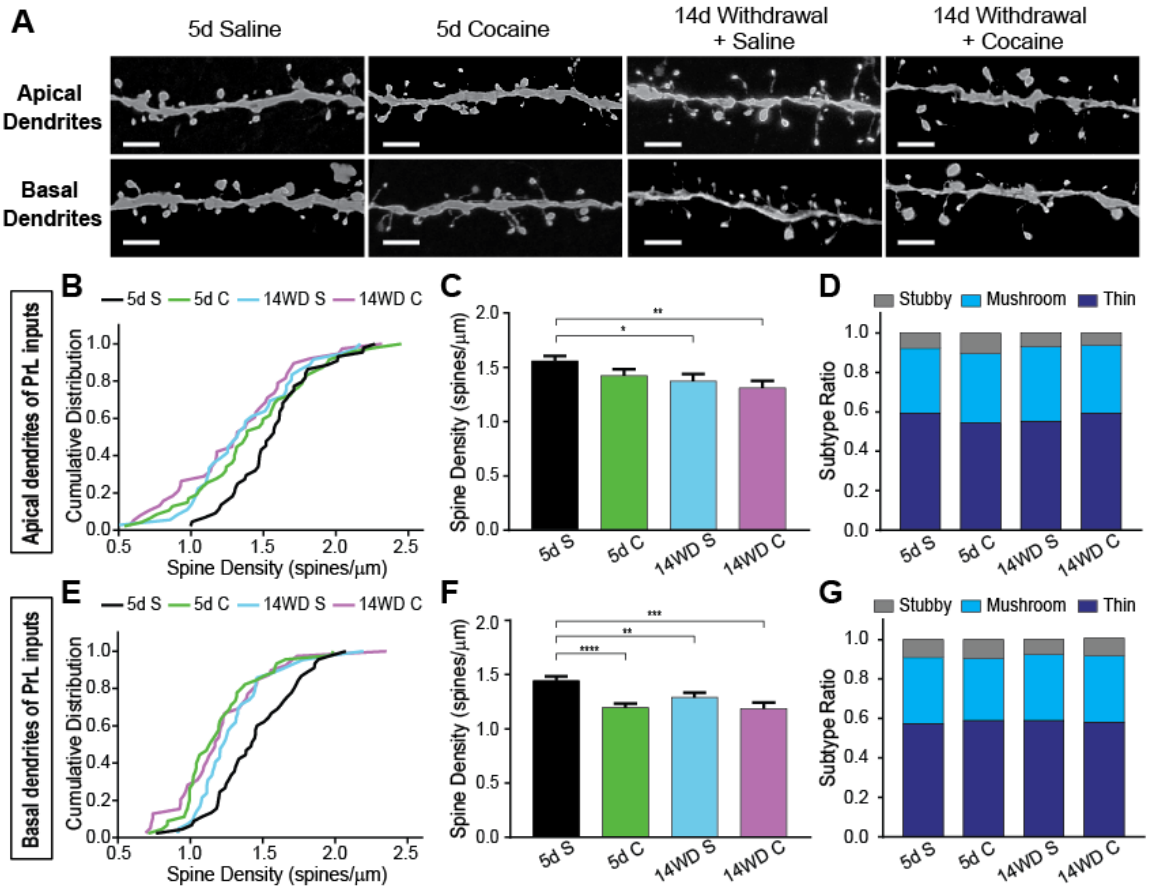

Figure 5. Spine densities of PrL neurons projecting to D1-MSNs decrease with cocaine exposure, withdrawal, and reinstatement. **A**) Sample images of apical (top) and basal (bottom) dendrites from PrL neurons projecting to D1-MSNs in different stages of cocaine administration. Scale bars represent 1 µm. **B**) Cumulative distribution of apical spine density of PrL neurons projecting to D1-MSNs (5d S: n = 44; 5d C: n = 47, p = 0.1575; 14WD S: n = 36, p = 0.0387; 14WD C: n = 38, p = 0.0235 when compared to 5d S); K-S test. **C**) Average spine density of dendritic spines analyzed in **B** with s.e.m (5d S: 1.56 ± 0.04531; 5d C: 1.422 ± 0.06241, p = 0.0885; 14WD S: 1.374 ± 0.06288, p = 0.0216; 14WD C: 1.309 ± 0.06762, p = 0.0038 when compared to 5d S, Mann-Whitney test. **D**) Stacked column chart depicting changes in average apical spine subtype ratios of PrL neurons projecting to D1-MSNs (5d S: n = 35; 5d C: n = 37; 14WD S: n = 36; 14WD C: n = 38). **E**) Cumulative distribution of basal spine density on PrL neurons projecting to D1-MSNs (5d S: n = 45; 5d C: n = 45, p = 0.0007.; 14WD S: n = 42, p = 0.0491, 14WD C: n = 40, p = 0.0008. when compared to 5d S); K-S test. **F**) Average spine density of dendritic spines analyzed in **E** with s.e.m (5d S: 1.443 ± 0.04362; 5d C: 1.193 ± 0.04149, p < 0.0001; 14WD S: 1.291 ± 0.04136, p = 0.0066; 14WD C: 1.186 ± 0.05534, p = 0.0002. **G**) Stacked column chart depicting changes in average basal spine subtype ratios of PrL neurons projecting to D1-MSNs (5d S: n = 37; 5d C: n = 34; 14WD S: n = 35; 14WD C: n = 40). Each n signifies a dendrite analyzed from 4-6 animals. *p<0.05, **p<0.005, ****p<0.0001

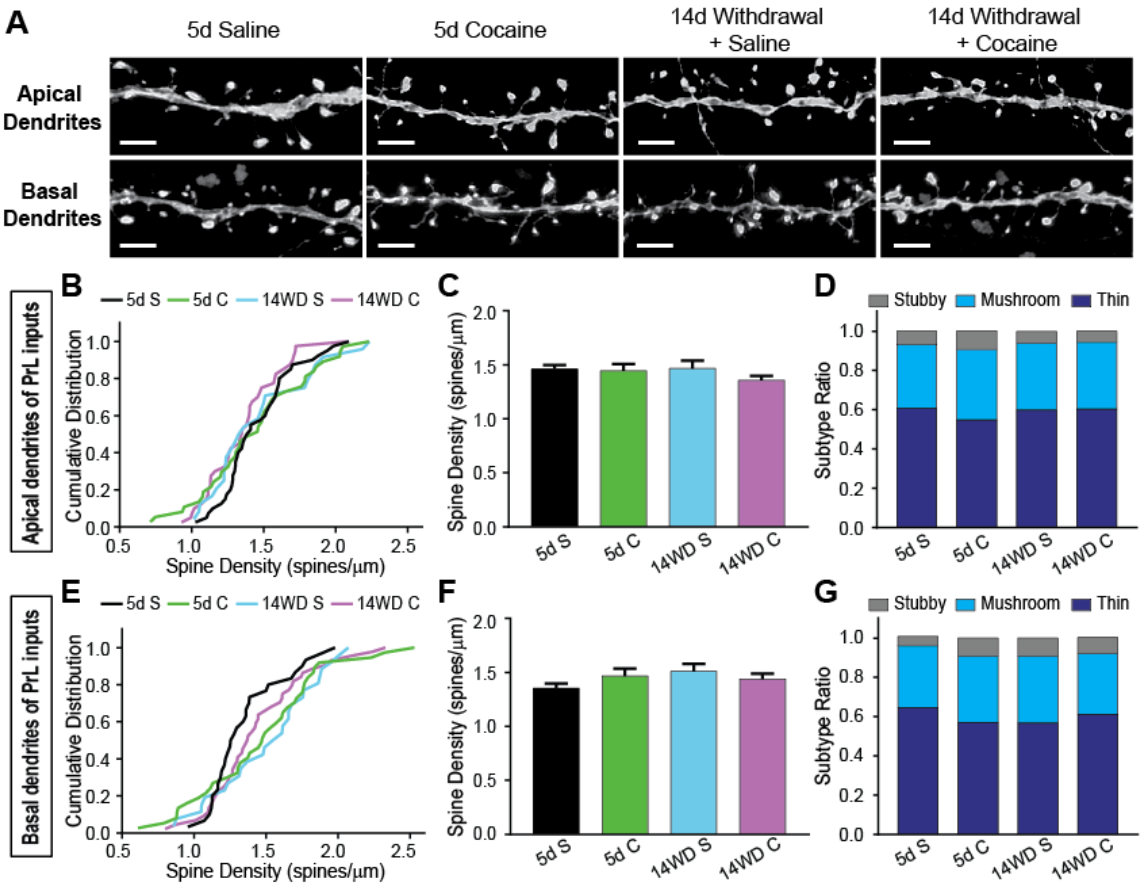

Figure 6. PrL neurons projecting to D2-MSNs show no change in spine densities irrespective of experimental group; however, thin and stubby spine ratios differ. **A**) Sample images of apical (top) and basal (bottom) dendrites from PrL neurons projecting to D2-MSNs in different stages of cocaine administration. Scale bars represent 1 µm. **B**) Cumulative distribution of apical spine density on PrL neurons projecting to D2-MSNs (5d S: n = 40; 5d C: n = 37, p = 0.5884; 14WD S: n = 24, p = 0.4334; 14WD C: n = 40, p = 0.2634 when compared to 5d S); K-S test. **C**) Average spine density of dendritic spines analyzed in **B** with s.e.m (5d S: 1.459 ± 0.03978; 5d C: 1.444 ± 0.06153, p = 0.7265; 14WD S: 1.466 ± 0.07216, p = 0.5308; 14WD C: 1.358 ± 0.03984, p = 0.1052 when compared to 5d S, Mann-Whitney test. **D**) Stacked column chart depicting changes in average apical spine subtype ratios of PrL neurons projecting to D2-MSNs (5d S: n = 31; 5d C: n = 37; 14WD S: n = 18; 14WD C: n = 33). **E**) Cumulative distribution of basal spine density on PrL neurons projecting to D2-MSNs (5d S: n = 30; 5d C: n = 37, p = 0.0567; 14WD S: n = 26, p = 0.0676, 14WD C: n = 44, p = 0.4074. when compared to 5d S); K-S test. **F**) Average spine density of dendritic spines analyzed in **E** with s.e.m (5d S: 1.352 ± 0.04729; 5d C: 1.466 ± 0.07062, p = 0.1932; 14WD S: 1.511 ± 0.0688, p = 0.0745; 14WD C: 1.438 ± 0.05086, p = 0.2382. **G**) Stacked column chart depicting changes in average basal spine subtype ratios of PrL neurons projecting to D2-MSNs (5d S: n = 30; 5d C: n = 37; 14WD S: n = 26; 14WD C: n = 36). Each n signifies a dendrite analyzed from 4-6 animals. Mann-Whitney test. *p<0.05, **p<0.005, ****p<0.0001

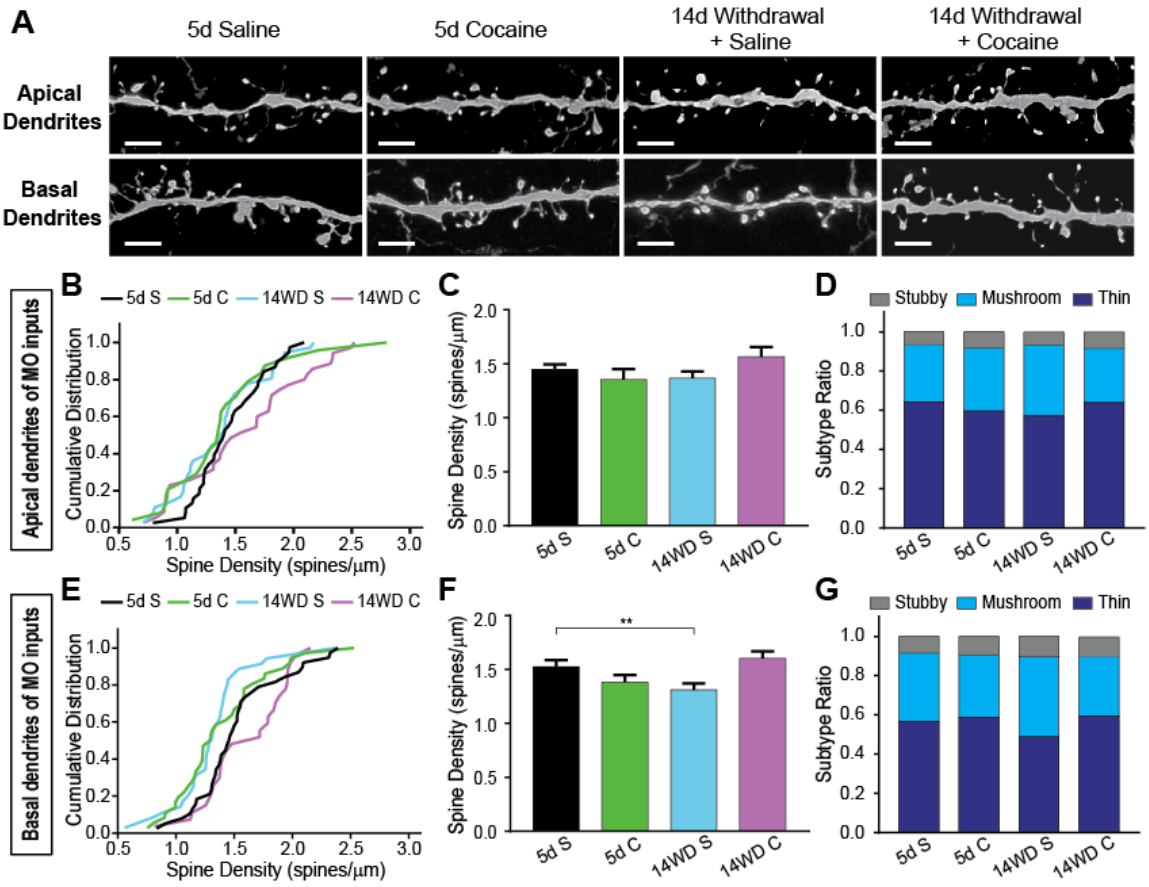

Figure 7. Basal, but not apical, dendrites of MO neurons projecting to D1-MSNs exhibit decreased spine density after cocaine withdrawal. **A**) Sample images of apical (top) and basal (bottom) dendrites from MO neurons projecting to D1-MSNs in different stages of cocaine administration. Scale bars represent 1 µm. **B**) Cumulative distribution of apical spine density of MO neurons projecting to D1-MSNs (5d S: n = 38; 5d C: n = 25, p = 0.2863; 14WD S: n = 36, p = 0.2843; 14WD C: n = 35, p = 0.2359 when compared to 5d S); K-S test. **C**) Average spine density of dendritic spines analyzed in **B** with s.e.m (5d S: 1.447 ± 0.04884; 5d C: 1.354 ± 0.09905, p = 0.2427; 14WD S: 1.366 ± 0.06395, p = 0.2837; 14WD C: 1.565 ± 0.08921, p = 0.3587 when compared to 5d S, Mann-Whitney test. **D**) Stacked column chart depicting changes in average apical spine subtype ratios of MO neurons projecting to D1-MSNs (5d S: n = 33; 5d C: n = 23; 14WD S: n = 36; 14WD C: n = 35). **E**) Cumulative distribution of basal spine density of MO neurons projecting to D1-MSNs (5d S: n = 38; 5d C: n = 36, p = 0.0484; 14WD S: n = 35, p = 0.0203, 14WD C: n = 27, p = 0.1001 when compared to 5d S); K-S test. **F**) Average spine density of dendritic spines analyzed in **E** with s.e.m (5d S: 1.524 ± 0.06108; 5d C: 1.383 ± 0.0659, p = 0.0846; 14WD S: 1.312 ± 0.05757, p = 0.0064; 14WD C: 1.603 ± 0.06673, p = 0.4080. **G**) Stacked column chart depicting changes in average basal spine subtype ratios of PrL neurons projecting to D1-MSNs (5d S: n = 33; 5d C: n = 31; 14WD S: n = 35; 14WD C: n = 27). Each n signifies a dendrite analyzed from 4-6 animals. *p<0.05, **p<0.005, ****p<0.0001

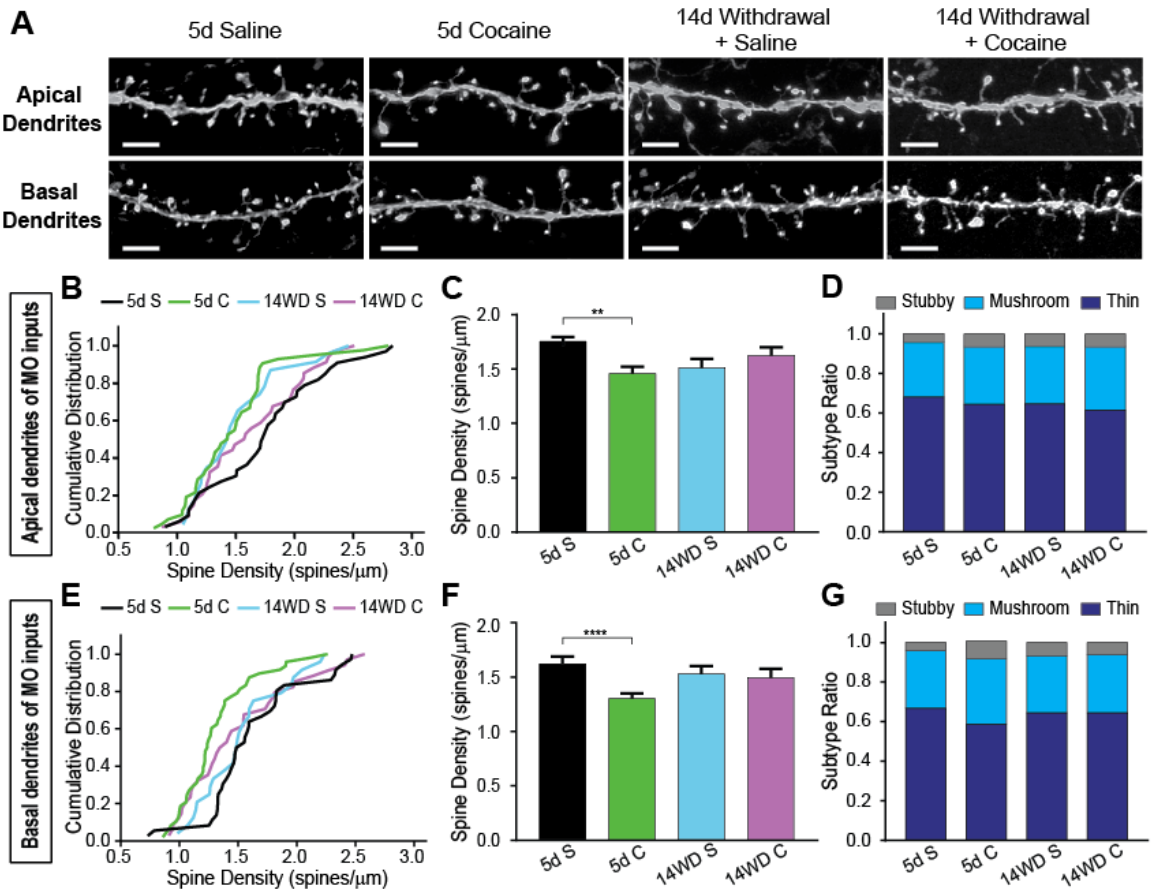

Figure 8. MO neurons projecting to D2-MSNs decrease in spine density with 5 days of cocaine exposure, but this change is extinguished after withdrawal and reinstatement. **A**) Sample images of apical (top) and basal (bottom) dendrites from MO neurons projecting to D1-MSNs in different stages of cocaine administration. Scale bars represent 1 µm. **B**) Cumulative distribution of apical spine densities of MO neurons projecting to D2-MSNs (5d S: n = 33; 5d C: n = 42, p = 0.0009; 14WD S: n = 23, p = 0.0938; 14WD C: n = 34, p = 0.5285 when compared to 5d S); K-S test. **C**) Average spine density of dendritic spines analyzed in **B** with s.e.m (5d S: 1.752 ± 0.08778; 5d C: 1.46 ± 0.06258, p = 0.0039; 14WD S: 1.512 ± 0.08113, p = 0.0642; 14WD C: 1.626 ± 0.07532, p = 0.3590 when compared to 5d S, Mann-Whitney test. **D**) Stacked column chart depicting changes in average apical spine subtype ratios of MO neurons projecting to D1-MSNs (5d S: n = 30; 5d C: n = 36; 14WD S: n = 23; 14WD C: n = 33). Mann-Whitney test. **E**) Cumulative distribution of basal spine density of MO projections (5d S: n = 36; 5d C: n = 48, p < 0.0001.; 14WD S: n = 24, p = 0.4756, 14WD C: n = 34, p = 0.0427. when compared to 5d S). **F**) Average spine density of dendritic spines analyzed in **E** with s.e.m (5d S: 1.62 ± 0.0705; 5d C: 1.304 ± 0.0453, p < 0.0001; 14WD S: 1.528 ± 0.07289, p = 0.4224; 14WD C: 1.495 ± 0.08104, p = 0.0789. **G**) Stacked column chart depicting changes in average basal spine subtype ratios of MO neurons projecting to D2-MSNs (5d S: n = 30; 5d C: n = 36; 14WD S: n = 24; 14WD C: n = 34). Each n signifies a dendrite analyzed from 4-6 animals. Mann-Whitney test. *p<0.05, **p<0.005, ****p<0.0001

Tables

Table 1. Summary table depicting dendritic spine density of neurons projecting to D1- or D2-MSNs of the NAc in the BLA, VH, PrL, and MO that reached statistically significant differences compared to control.

			5D C	14WD S	14WD C
BLA	D1		↑	↑	↑
	D2				
VH	D1	Apical			↑
		Basal			↑
	D2	Apical			
		Basal			
PrL	D1	Apical		↓	↓
		Basal	↓	↓	↓
	D2	Apical			
		Basal			
MO	D1	Apical			
		Basal		↓	
	D2	Apical	↓		
		Basal	↓		

Table 2. Summary table depicting dendritic spine subtype ratios of neurons projecting to D1- or D2-MSNs of the NAc in the BLA, VH, PrL, and MO that reached statistically significant differences compared to control.

			Thin			Mushroom			Stubby		
			5D C	14WD S	14WD C	5D C	14WD S	14WD C	5D C	14WD S	14WD C
BLA	D1			↓	↓		↑	↑			
	D2			↑		↓	↓	↓	↑		↑
VH	D1	Apical									
		Basal								↓	↓
	D2	Apical									
		Basal	↓								
PrL	D1	Apical							↑		
		Basal									
	D2	Apical	↓						↑		
		Basal	↓						↑	↑	↑
MO	D1	Apical		↓			↑				
		Basal					↑				
	D2	Apical	↓						↑	↑	↑
		Basal	↓						↑	↑	↑

Graphs

Graph 1. Cocaine-induced behavioral sensitization. Locomotion was measured for 15 minutes after each saline or cocaine injection and separated in graphs by genotype (D1- or A2a-cre) and cocaine exposure groups. **A**) Locomotor data for D1-cre animals exposed to 5 days of saline (n = 5) and 5 days of cocaine (n = 6). **B**) Locomotor data for D1-cre animals exposed to 5 days of cocaine after a 14 day withdrawal, followed by a saline reinstatement (n = 7) or a cocaine reinstatement (n = 10). **C**) Locomotor data for A2a-cre animals exposed to 5 days of saline (n = 6) and 5 days of cocaine (n =5). **D**) Locomotor data for A2a-cre animals exposed to 5 days of cocaine after a 14 day withdrawal, followed by a saline reinstatement (n = 3) or a cocaine reinstatement (n = 4).

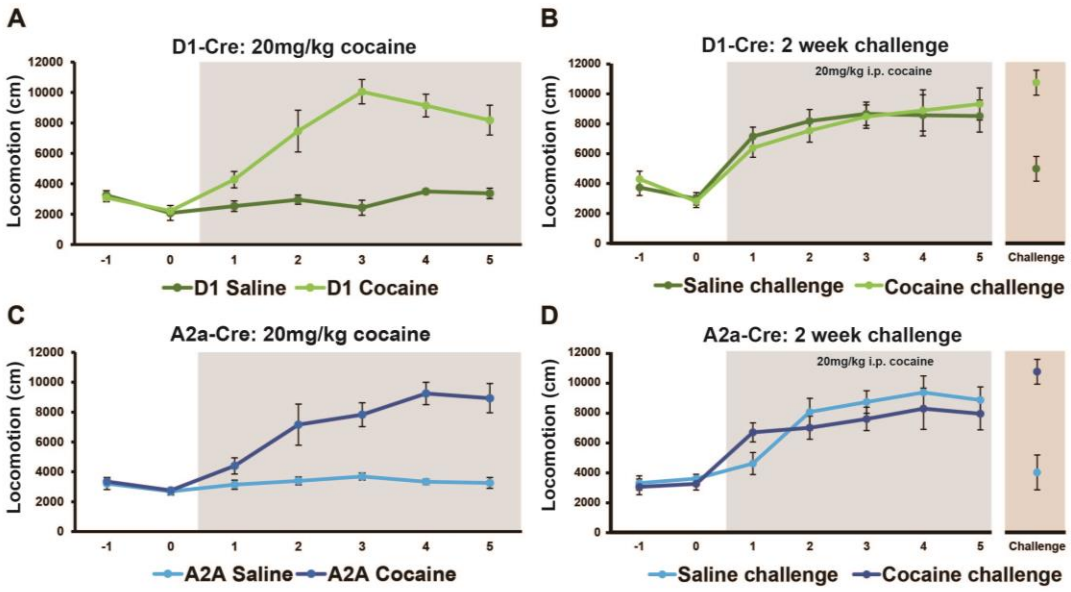

Discussion

The ability of cocaine to change spine densities and modify synaptic plasticity is not specific to the NAc. It appears that cocaine is also able to induce effects in other brain areas, however in an extremely selective manner; the kind of cocaine-induced structural changes is dependent on the brain area the neurons are in, whether it projects to D1 or D2-MSNs of the NAc, and what stage of cocaine exposure the animal is in.

BLA neurons projecting to D1-MSNs exhibit an increasing spine density after 5 days of cocaine administration, with a further increase even after 14 days of withdrawal and a saline challenge. This indicates cocaine exposure may be increasing the amount of excitatory synapses onto BLA neurons – an area associated with emotion-driven behaviors – leading to increased likelihood of pursuing appetitive behaviors after initial use. The increasing amount of excitatory inputs to D1-MSN projecting BLA neurons after 14 days of withdrawal suggests it is even likelier to engage in appetitive pursuits. Studies showed that activation of NAc projecting BLA neurons facilitates cocaine seeking (Hayes 2003). It is possible that newly generated spines on D1-MSN projecting BLA neurons contribute to cocaine seeking, and the high degree of relapse in human addicts (McLellan 2000). Once given a cocaine challenge after a 14 day withdrawal, these BLA neurons undergo structural plasticity that leaves it at similarly heightened levels after the initial 5 days of cocaine injections. It may be that cocaine exposure induces a new baseline level of dendritic spine density in

the D1-MSN projecting BLA neurons, irrespective of whether it is initial cocaine administration or as reinstatement.

Interestingly, a decreasing proportion of thin spines are replaced by mushroom spines after 14 days of withdrawal, with either a saline or cocaine challenge. During the withdrawal period, D1-MSN projecting BLA neurons may either reuptake thin spines and create new mushroom spines, or allow thin spines to mature into mushroom spines. This can be consistent with an increase in excitatory inputs to these BLA neurons, as mushroom spines are considered to have greater synaptic strength than thin spines, leading to an overall increase in excitability of the neurons (Hering 2001).

Despite robust changes in spine density and subtype ratios in BLA neurons that project to D1-MSNs, none of the cocaine-exposed animals show any changes in dendritic spine density of BLA neurons projecting to D2-MSNs. This supports the hypothesis that there may be a dysregulation in the activity of D1- and D2-MSNs in drug addiction, as D1-MSNs are likely to be activated more if neurons sending excitatory inputs to them are also receiving more excitatory synaptic inputs. However, a similar spine density does not mean the same synaptic projections to these D2-MSN projecting BLA neurons are necessarily retained. There is a decrease in mushroom subtypes, replaced by thin spines after 14 days of withdrawal, or by stubby spines after 5 days of cocaine and a 14 day withdrawal with cocaine challenge. This indicates a preference for increasing stubby spines in animals exposed to cocaine within the past day, but not those

exposed two weeks prior. These findings show a new level of cocaine-induced changes, as a previous report indicated cocaine-induced structural plasticity changes only in thin spines in the NAc (Dumitriu 2012).

VH neurons projecting to D1-MSNs has a much less prominent change in both apical and basal dendrites, as there is a trend towards increased spine density after a 14 day withdrawal and saline challenge, and reaches a significant increase after a cocaine reinstatement shot. This may reflect structural plasticity changes solely from re-exposure to cocaine.

As with the BLA neurons, VH neurons projecting to D2-MSNs exhibit no significant difference in dendritic spine density in any cocaine-exposed groups compared to control. This phenomenon may further contribute to dysregulation of D1- and D2-MSN activity, as D1-MSNs are comparatively more likely to be activated than D2-MSNs compared to animals not exposed to cocaine reinstatement.

The PrL, associated with higher cognition and self-control, is a probable candidate for a weakening effect by cocaine – given that those who are addicted struggle to maintain self-control. Indeed, our data support this possibility. In contrast to the BLA and VH neurons, PrL neurons projecting to D1-MSNs exhibit a decreasing dendritic spine density with cocaine exposure that is unrecovered even after a 2 week withdrawal in both apical and basal dendrites, although 5d cocaine administration didn’t induce significant change in the dendritic spines of the apical dendrites. Interestingly, the only spine subtype ratio changes we

observe is after 5 days of cocaine, as there is an increase in stubby spines in the apical dendrites. Aside from that, cocaine exposure appears to nonspecifically induce pruning of all spine subtypes in both apical and basal dendrites.

Following the trend thus far, PrL neurons projecting to D2-MSNs do not experience significant changes in dendritic spine density. However, there is some spine rearrangement occurring: the apical dendrites of PrL neurons projecting to D2-MSNs exhibits an increase in stubby spines, replacing the decreasing ratio of thin spines only after initial 5 day cocaine exposure. The basal dendrites exhibit an increase in stubby spines across all cocaine-exposed groups. Given the increase in stubby spines in many brain areas after cocaine exposure, there may be a greater significance to the function of stubby spines in addiction pathology than previously noted.

Because of functional differences, we believed that the PrL and MO of the prefrontal cortex may be affected differentially by cocaine exposure. This turned out to be the case, as the MO obtains very few dendritic spine density changes after cocaine exposure, as only basal dendrites in a two week withdrawal experience a decrease in spine density. The proportion of MO activity and cocaine craving has been found in human addicts (Volkow and Folwer 2000); interestingly, our data contrasts this as rodents undergoing 14 days of cocaine withdrawal experience a decreased spine density in both dendritic subtypes of neurons projecting to NAc D1-MSNs, suggesting lower activation of MO neurons projecting to D1-MSNs. The MO is also the only brain area studied that exhibits

decreases in neurons projecting to D2-MSNs; this decrease occurs only after initial 5 days of repetitive cocaine use.

In almost all cases, cocaine exposure modifies spine densities on neurons projecting to NAc D1-MSNs, but not D2-MSNs. First, this is consistent with findings that cocaine induced changes in NAc D1-MSNs that are not seen in D2-MSNs (MacAskill 2014). Second, cocaine appears to predominantly alter both D1-MSNs and projections to it, likely contributing to dysregulated activity of the NAc MSN subtypes leading to addiction. Though previous reports implicate thin spines primarily in cocaine induced spine density changes of the NAc, we show that the main excitatory projections to the NAc may undergo changes in the ratio of all three spiny subtypes (Dumitriu 2012). This suggests a greater possible importance in mushroom and stubby spines in the progression to addiction than previously believed.

The progression to drug addiction initiates as recreational use that evolves into compulsive use (Everitt 2005); the VH is likely a structure mediating some of the changes in this progression, as it encodes contextual cues related to cocaine intake and leads to cue-induced cocaine relapse (Lasseter 2010). Forced abstinence from cocaine progressively increases cue-induced craving in rodents, leading cravings to be higher after 6 months than in the first days of withdrawal (Wolf 2016). This delay in dendritic spine density changes in the VH, occurring only after a two week withdrawal, may underlie some of the behavioral phenotypes leading to the switch from drug use to addiction.

Addiction is an emotion-driven behavior with little regard for consequences or behavior considered unacceptable. Therefore, one may predict this dysregulation is due to a decrease in executive control of the cortex that is now unable to facilitate self-control in an individual. Instead, this control is shifted from the PFC to amygdalar regions which are involved in emotional behaviors. Our data showing cocaine-induced increases in spine density of BLA neurons projecting to NAc D1-MSNs provide support for the theory of a decrease in PFC control over behavior that is passed onto the BLA, leading to an increase in emotion-guided actions toward appetitive behaviors by those afflicted with a drug addiction.

Our results indicate the ability of cocaine to induce structural plasticity in a complex manner, dependent on the region of the excitatory afferents, the cell types in the NAc these neurons project to, and the stage of cocaine exposure the animal is in. Furthermore, alterations in stubby and mushroom spines implicate these subtypes, in addition to thin spines, as relevant players in the progression to drug addiction. These findings set up a foundation upon which further research may build on to increase our knowledge of the mechanisms and dysregulation leading from recreational drug use to the progression to drug addiction, such that effective drug addiction treatments can finally be developed.

References

1. Bechara A, Damasio AR, Damasio H, Anderson SW (1994) Insensitivity to future consequences following damage to human prefrontal cortex. *Cognition* 50: 7-15.

2. Britt JP, Benaliouad F, McDevitt RA, Stuber GD, Wise RA, Bonci A (2012) Synaptic and Behavioral Profile of Multiple Glutamatergic Inputs to the Nucleus Accumbens. *Neuron* 76(4): 790-803.

3. Chen BT, Yau HJ, Hatch C, Kusumoto-Yoshida I, Cho SL, Hopf FW, Bonci A. Rescuing cocaine-induced prefrontal cortex hypoactivity prevents compulsive cocaine seeking. *Nature Letters* 496 (7445): 359-362.

4. Dackis CA, O'Brien CP (2001). Cocaine dependence: a disease of the brain's reward centers. *Journal of Substance Abuse Treatment* 21(3): 111-117.

5. Dumitriu D, LaPlant Q, Grossman YS, Dias C, Janssen WG, Russo SJ, Morrison JH, Nestler EJ (2012) Subregional, Dendritic Compartment, and Spine Subtype Specificity in Cocaine Regulation of Dendritic Spines in the Nucleus Accumbens. *The Journal of Neuroscience* 32(20): 6957-6966.

6. Everitt BJ, Robbins TW (2005) Neural systems of reinforcement for drug addiction: from actions to habits to compulsion. *Nature Neuroscience* 8(1): 1481-1489.

7. Fuchs RA, Weber SM, Neisewander JL (2002) Effects of excitotoxic lesions of the basolateral amygdala on cocaine-seeking behavior and cocaine conditioned place preference in rats. *Brain Research* 929(1): 15-25.

8. Gerfen CR, Surmeier DJ (2011) Modulation of striatal projection systems by dopamine. *Annual Review of Neuroscience* 34: 441-466.

9. Hayes RJ, Vorel SR, Spector J, Liu X, Gardner EL (2003) Electrical and chemical stimulation of the basolateral complex of the amygdala reinstates cocaine-seeking behavior in the rat. *Psychopharmacology* 168: 75-83.

10. Hering H and Sheng M (2001). Dendritic spines: structure, dynamics, and regulation. *Nature Reviews Neuroscience* 2:880-888.

11. Johnson LD, O'Malley PM, Bachman JG, Schulenberg JE, Miech RA (2015) Monitoring the Future National Survey Results on Drug Use, 1975-2014: Volume 2. College students and adults ages 19-55. *Ann Arbor, MI: Institute for Social Research, The University of Michigan*, pp 385.

12. Kantak KM, Black Y, Valencia E, Green-Jordan K, Eichenbaum HB (2002) Dissociable Effects of Lidocaine Inactivation of the Rostral and Caudal Basolateral Amygdala on the Maintenance and Reinstatement of Cocaine-Seeking Behavior in Rats. *The Journal of Neuroscience* 22(3): 1126-1136.

13. Kupchik YM, Brown RM, Heinsbroek JA, Lobo MK, Schwartz DJ, Kalivas PW (2015) Coding the direct/indirect pathways by D1 and D2 receptors is not valid for accumbens projections. *Nature Neuroscience* 18:9 1230-1232.

14. Lasseter HC, Xie X, Ramirez DR, Fuchs RA (2010) Sub-region specific contribution of the ventral hippocampus to drug context-induced reinstatement of cocaine-seeking behavior in rats. *Neuroscience* 171(3): 830-839.

15. Li XG, Somogyi P, Ylinen A, Buzsaki G (1994) The hippocampal CA3 network: An in vivo intracellular labeling study. *Journal of Comparative Neurology* 339:2 181-208.

16. Li Y, Acerbo MJ, Robinson TE (2004) The induction of behavioural sensitization is associated with cocaine-induced structural plasticity in the core (but not shell) of the nucleus accumbens. *European Journal of Neuroscience* 20(6): 1647-1654.

17. Lobo MK, Covington HE 3rd, Chaudhury D, Friedman AK, Sun H, Damez-Werno D, Dietz DM, Zaman S, Koo JW, Kennedy PK, Mouzon E, Mogri M, Neve RL, Deisseroth K, Han MH, Nestler EJ (2010) Cell type-specific loss of BDNF signaling mimics optogenetic control of cocaine reward. *Science* 330(6002): 385-90.

18. MacAskill AF, Cassel JM, Carter AG (2014) Cocaine exposure reorganizes cell type- and input- specific connectivity in the nucleus accumbens. *Nature Neuroscience*. 17(9) 1198-1207.

19. Mar AC, Walker AL, Theobald DE, Eagle DM, Robbins TW (2011) Dissociable Effects of Lesions to Orbitofrontal Cortex Subregions on

Impulsive Choice in the Rat. *The Journal of Neuroscience* 31(17): 6398-6404.

20. Matochik JA, London ED, Eldreth DA, Cadet JL, Bolla KI (2003) Frontal cortical tissue composition in abstinent cocaine abusers: a magnetic resonance imaging study. *NeuroImage* 19(3): 1095-1102.

21. McClure SM, Laibson DI, Loewenstein G, Cohen JD (2004) Separate Neural Systems Value Immediate and Delayed Monetary Rewards. *Science* 306: 503-507.

22. McLellan AT, Lewis DC, O'Brien CP, Kleber HD (2000) Drug dependence, a chronic medical illness: implications for treatment, insurance, and outcomes evaluation. *The Journal of the American Medical Association* 284(13): 1689-1695.

23. Miller CA and Marshall JF (2004) Altered Prelimbic Cortex Output during Cue-elicited Drug Seeking. *The Journal of Neuroscience* 24(31): 6889-6897.

24. Olds J and Milner P (1954) Positive reinforcement produced by electrical stimulation of septal area and other regions of rat brain. *Journal of Comparative and Physiological Psychology* 47(6):419-27.

25. Pelloux Y, Murray JE, Everitt BJ (2013) Differential roles of the prefrontal cortical subregions and basolateral amygdala in compulsive cocaine seeking and relapse after voluntary abstinence in rats. *European Journal of Neuroscience* 38(7): 3018-3026.

26. Penzes P, Cahill ME, Jones KA, Vanleeuwen J, Woolfrey KM (2011) Dendritic spine pathology in neuropsychiatric disorders. *Nature Neuroscience* 14: 285-293.

27. Pierce RC, Reeder DC, Hicks J, Morgan ZR, Kalivas PW (1997) Ibotenic acid lesions of the dorsal prefrontal cortex disrupt the expression of behavioral sensitization to cocaine. *Neuroscience* 82:4 1103-1114.

28. Richard JM, Berridge KC (2011) Nucleus Accumbens Dopamine/Glutamate Interaction Switches Modes to Generate Desire versus Dread: D1 Alone for Appetitive Eating but D1 and D2 Together for Fear. *The Journal of Neuroscience* 31(36): 12866-12879

29. Rodriguez A, Ehlenbeger DB, Dickstein DL, Hof PR, Wearne SL (2008). Automated Three-Dimensional Detection and Shape Classification of Dendritic Spines from Fluorescence Microscopy Images. *PLoS ONE* 3(4): e1997.

30. Rosenkranz JA, Grace AA (2002) Cellular Mechanisms of Infralimbic and Prelimbic Prefrontal Cortical Inhibition and Dopaminergic Modulation of Basolateral Amygdala Neurons In Vivo. *The Journal of Neuroscience* 22(1): 324-337.

31. Steketee JD (2005) Cortical Mechanisms of Cocaine Sensitization. *Critical Reviews in Neurobiology* 17(2): 69-86.

32. Stuss DT and Levine B (2002) Adult Clinical Neuropsychology: Lessons from Studies of the Frontal Lobes. *Annual Reviews of Psychology* 53: 401-433.

33. Sun W and Rebec GV (2003). Lidocaine Inactivation of Ventral Subiculum Attenuates Cocaine-Seeking Behavior in Rats. *The Journal of Neuroscience* 23(32): 10258-10264.

34. Tzschentke TM, Schmidt WJ (1998) Discrete quinolinic acid lesions of the rat prelimbic medial prefrontal cortex affect cocaine- and MK-801-, but not morphine- and amphetamine-induced reward and psychomotor activation as measured with the place preference conditioning paradigm. *Behavioural Brain Research* 97: 115-127.

35. Tzschentke TM, Schmidt WJ (1998) The development of cocaine-induced behavioral sensitization is affected by discrete quinolinic acid lesions of the prelimbic medial prefrontal cortex. *Brain Research* 795(1-2): 71-76.

36. Volkow ND and Fowler JS (2000) Addiction, a disease of compulsion and drive: Involvement of the orbitofrontal cortex. *Cerebral Cortex* 10(3): 318-325.

37. Vorel SR, Liu X, Hayes RJ, Spector JA, Gardner EL (2001) Relapse to Cocaine-Seeking After Hippocampal Theta Burst Stimulation. *Science* 292(5519): 1175-1178.

38. Winstanley CA, Bachtell RK, Theobald DE, Laali S, Green TA, Kumar A, Chakravarty S, Self DW, Nestler EJ (2009) Increased Impulsivity during Withdrawal from Cocaine Self-Administration: Role for ΔFosB in the Orbitofrontal Cortex. *Cerebral Cortex* 19: 435-444.

39. Wolf ME (2016) Synaptic mechanisms underlying persistent cocaine craving. *Nature Reviews Neuroscience* 17: 351-365.